University of Wisconsin - Madison

MADPH-95-868

October 1995

Fermion confinement by a relativistic flux tube

M.G. Olsson and Siniša Veseli

Department of Physics, University of Wisconsin, Madison, WI 53706

Ken Williams

Continuous Electron Beam Accelerator Facility

Newport News, VA 29606, USA

and

Physics Department, Hampton University, Hampton, VA 29668

Abstract

We formulate the description of the dynamic confinement of a single fermion by a flux tube. The range of applicability of this model extends from the relativistic corrections of a slowly moving quark to the ultra-relativistic motion in a heavy-light meson. The reduced Salpeter equation, also known as the no-pair equation, provides the framework for our discussion. The Regge structure is that of a Nambu string with one end fixed. Numerical solutions are found giving very good fits to heavy-light meson masses. An Isgur-Wise function with a zero recoil slope of $\xi'(1) \simeq -1.26$ is obtained.

1 Introduction

The relativistic flux tube (RFT) model's [1] major success has been its ability to account for leading relativistic corrections in heavy quark bound states and also to give the Regge structure of the Nambu string. The "Wilson loop low velocity expansion" of Eichten and Feinberg [2] provides a rigorous non-perturbative framework for the discussion of these corrections. The spin-independent relativistic corrections were computed in an extension of this program [3]. The spin-independent QCD relativistic corrections are accounted for in a simple dynamical picture by the RFT model [4]. The spin-dependent long range corrections have also been considered in the RFT model [5]. In the present work we show that the spin-orbit interaction obtained as a relativistic correction, differs from the "Thomas term" conventionally associated with QCD [6].

Yet to be completely explored is the ultra-relativistic sector of the RFT model with fermions, although the spinless quark results have been encouraging [1, 7, 8]. In fact, with reasonable assumptions the Wilson area law exactly reproduces the original spinless RFT model [9, 10]. One of the attractive features of the RFT model is that ultra-relativistic quark motion has little influence on meson's rotational dynamics. For large angular momenta the tube's momentum and energy dominate and the RFT reduces to the Nambu string. The RFT flux tube can also stretch radially which involves no change in tube's momentum. For s-waves it then resembles a potential model. If both radial and angular motions are present Coriolis force couples the radial and rotational motions and implies a straight leading Regge trajectory accompanied by parallel equally spaced daughter trajectories [1, 7].

In recent work [11] we have examined the motion of a fermion in a confining central potential field and found that the Dirac equation is appropriate for scalar confinement while the "no-pair" variant of the Dirac equation (or reduced Salpeter equation), must be used for a Lorentz vector confining potential. Since the RFT acts like vector confinement for low angular momenta the Salpeter equation is relevant.

Our formalism for fermionic quark confinement is unusual in that the confinement is introduced into the kinetic rather than in the usual interaction term. The flux tube contributes to both energy and momentum to the dynamics so it makes little sense to consider it as a "potential" type interaction. By a covariant substitution we add the tube to the quark momentum and energy. We may equivalently view this as a "minimal substitution" of a vector interaction field. The result nicely reduces to the Nambu string in the limit in which the quark moves ultra-relativistically.

In Section 2 we discuss the quantized form of the tube operator and the flux tube transformation. Starting from the reduced Salpeter (or no-pair) equation, we develop the radial equations with tube confinement in Section 3. A semi-relativistic reduction is presented in Section 4. In Section 5 the Regge structure of the RFT model for an ultra-relativistic fermion is determined, yielding a straight trajectory with slope $\alpha' = \frac{1}{\pi a}$. In Section 6 we present our numerical results. We obtain an excellent fit to the observed particle spectrum and compute the Isgur-Wise function for the semileptonic $\bar{B} \to D^{(*)} l \bar{\nu}_l$ decays. Our conclusions are found in Section 7.

2 Flux tube transformation

From the Lagrangian formulation of the spinless RFT model [1] it follows that the canonical linear momentum is sum of quark and the tube parts

$$\mathbf{p} \;=\; \mathbf{p}_q + \mathbf{p}_t \;, \tag{1}$$

where

$$p_q \;=\; \frac{L_q}{r} = W_r \gamma_\perp v_\perp \;, \tag{2}$$

$$p_t \;=\; \frac{L_t}{r} = 2arF(v_\perp) \;, \tag{3}$$

with

$$F(v_\perp) = \frac{1}{4v_\perp}\left(\frac{\arcsin v_\perp}{v_\perp} - \frac{1}{\gamma_\perp}\right) \;, \tag{4}$$

and the tube energy is found to be

$$H_t = ar\frac{\arcsin v_\perp}{v_\perp} \ . \tag{5}$$

In these expressions $\gamma_\perp = \frac{1}{\sqrt{1-v_\perp^2}}$ and $W_r = \sqrt{p_r^2 + m^2}$.

In an earlier work [5] the flux tube with fermionic ends was introduced through the free Dirac Hamiltonian by the covariant transformation,

$$p^\mu \to p^\mu - p_t^\mu \ , \tag{6}$$

where

$$\begin{aligned} p_t^\mu &= (H_t, \mathbf{p}_t) \ , &(7)\\ \mathbf{p}_t &= (-\hat{\mathbf{r}} \times \hat{\mathbf{L}})p_t = -\hat{\mathbf{r}} \times \frac{\mathbf{L}_t}{r} \ . &(8) \end{aligned}$$

Here, unlike in [5], we want to quantize this classical transformation at the outset. The prescription we follow is to first quantize H_t, p_t, and p_q by symmetrization of the classical expressions [1, 8], so that

$$\begin{aligned} H_t &= \frac{a}{2}\{r, \frac{\arcsin v_\perp}{v_\perp}\} \ , &(9)\\ p_t &= \frac{L_t}{r} = a\{r, F(v_\perp)\} \ , &(10)\\ p_q &= \frac{L_q}{r} = \frac{1}{2}\{W_r, \gamma_\perp v_\perp\} \ , &(11) \end{aligned}$$

with $\{A, B\} = AB + BA$ and $p_r^2 = -\frac{1}{r}\frac{\partial^2}{\partial r^2}r$. The quantum operators corresponding to $\mathbf{p}_t$ and $\mathbf{p}_q$ are then

$$\begin{aligned} \mathbf{p}_t &= \frac{1}{2}(\frac{\mathbf{L}_t}{r} \times \hat{\mathbf{r}} - \hat{\mathbf{r}} \times \frac{\mathbf{L}_t}{r}) &(12)\\ \mathbf{p}_q &= \hat{\mathbf{r}}p_r + \frac{1}{2}(\frac{\mathbf{L}_q}{r} \times \hat{\mathbf{r}} - \hat{\mathbf{r}} \times \frac{\mathbf{L}_q}{r}) &(13) \end{aligned}$$

where $p_r = -\frac{i}{r}\frac{\partial}{\partial r}r$ is hermitian. From $\mathbf{p} = \mathbf{p}_q + \mathbf{p}_t$ and the identity

$$\hat{\mathbf{r}}p_r + \frac{1}{2}(\frac{\mathbf{L}}{r} \times \hat{\mathbf{r}} - \hat{\mathbf{r}} \times \frac{\mathbf{L}}{r}) = \hat{\mathbf{r}}(-i\frac{\partial}{\partial r}) - \hat{\mathbf{r}} \times \frac{\mathbf{L}}{r} \ , \tag{14}$$

we obtain the usual

$$\mathbf{p} \;=\; \hat{\mathbf{r}}(-i\frac{\partial}{\partial r}) - \hat{\mathbf{r}} \times \frac{\mathbf{L}}{r} \; . \tag{15}$$

The full flux tube transformation (6) of the free Dirac Hamiltonian is then given by

$$H_0(\mathbf{p}) \rightarrow H_0(\mathbf{p}) + H_t - \boldsymbol{\alpha} \cdot \mathbf{p}_t \;, \tag{16}$$

where

$$H_0(\mathbf{p}) = \boldsymbol{\alpha} \cdot \mathbf{p} + \beta m \; . \tag{17}$$

We choose to work with the reduced Salpeter equation [12, 13] in the limit where the heavy antiquark mass is infinite [14]. In coordinate space it is given by

$$\Lambda_+[E_q - H_0(\mathbf{p}) - V(r)]\Lambda_+\Psi(\mathbf{r}) = 0 \;, \tag{18}$$

and also known as the no-pair equation [15]. Here, $E_q = M - m_{\bar{Q}}$ is the energy of the light degrees of freedom, $V(r)$ is the short range vector interaction, while Λ_+ is the positive energy projection operator

$$\Lambda_+ = \frac{E_0 + H_0}{2E_0} \;, \tag{19}$$

with

$$E_0 = \sqrt{\mathbf{p}^2 + m^2} \; . \tag{20}$$

The flux-tube transformation (16) on equation (18) results in the no-pair equation describing heavy-light mesons with the flux tube accounting for the long range interaction

$$[E_q - H_0(\mathbf{p}) - \Lambda_+(V(r) + H_t - \boldsymbol{\alpha} \cdot \mathbf{p}_t)\Lambda_+]\Psi(\mathbf{r}) = 0 \; . \tag{21}$$

3 Radial equations

Coupled radial eigenvalue equations follow from the spherical symmetry of equation (21). As in [11] the solutions are of the form

$$\Psi^k_{jm}(\mathbf{r}) = \left(\begin{array}{c} f^k_j(r)\mathcal{Y}^k_{jm}(\hat{\mathbf{r}}) \\ ig^k_j(r)\mathcal{Y}^{-k}_{jm}(\hat{\mathbf{r}}) \end{array} \right) \equiv \mathbb{Y} \left(\begin{array}{c} f^k_j \\ g^k_j \end{array} \right) , \tag{22}$$

where

$$\mathbb{Y} = \left(\begin{array}{cc} \mathcal{Y}^k_{jm} & 0 \\ 0 & i\mathcal{Y}^{-k}_{jm} \end{array} \right) . \tag{23}$$

The Dirac quantum number k labels the bound state and is defined by [16]

$$k = \pm(j + \frac{1}{2}) . \tag{24}$$

The identities

$$\boldsymbol{\sigma} \cdot \mathbf{L}\mathcal{Y}^k_{jm} = -(k+1)\mathcal{Y}^k_{jm} , \tag{25}$$

$$\boldsymbol{\sigma} \cdot \hat{\mathbf{r}}\mathcal{Y}^k_{jm} = -\mathcal{Y}^{-k}_{jm} , \tag{26}$$

lead to

$$\boldsymbol{\sigma} \cdot \mathbf{p}\mathcal{Y}^{\pm k}_{jm}(\hat{\mathbf{r}}) = i\mathcal{Y}^{\mp k}_{jm}(\hat{\mathbf{r}})D_\pm , \tag{27}$$

$$\boldsymbol{\sigma} \cdot \mathbf{p}_t\mathcal{Y}^{\pm k}_{jm}(\hat{\mathbf{r}}) = \mp i\mathcal{Y}^{\mp k}_{jm}(\hat{\mathbf{r}})T_t , \tag{28}$$

where

$$D_\pm = \pm\frac{k}{r} + (\frac{\partial}{\partial r} + \frac{1}{r}) , \tag{29}$$

$$T_t = \frac{1}{2}\left[\frac{(1-k)}{\sqrt{-k(1-k)}}p_t^{-k} - \frac{(1+k)}{\sqrt{k(1+k)}}p_t^k\right] . \tag{30}$$

The no-pair equation can now be expressed in radial form. Starting from (21) and the wave function (22), we use the above relations to obtain matrix radial no-pair equations

$$(E_q - \mathbb{h}_0 - \mathbb{L}\mathbb{I}\mathbb{L}) \begin{pmatrix} f_j^k \\ g_j^k \end{pmatrix} = 0 \ , \tag{31}$$

with definitions

$$\mathbb{h}_0 \equiv \begin{pmatrix} m & -D_- \\ D_+ & -m \end{pmatrix} , \tag{32}$$

$$\mathbb{L} \equiv \begin{pmatrix} \lambda_+ & -\frac{1}{2E_0^+} D_- \\ D_+ \frac{1}{2E_0^+} & \lambda_- \end{pmatrix} , \tag{33}$$

$$\mathbb{I} \equiv \begin{pmatrix} V(r) + H_t^k & T_t \\ T_t & V(r) + H_t^{-k} \end{pmatrix} . \tag{34}$$

In the above expressions

$$\lambda_\pm = \frac{E_0^\pm \pm m}{2E_0^\pm} , \tag{35}$$

$$E_0^\pm = \sqrt{m^2 - D_\mp D_\pm} \ . \tag{36}$$

From (34) we observe that the tube energy enters much like the time component of the short range Lorentz vector potential $V(r)$, which we take to be

$$V(r) = -\frac{\kappa}{r} \ . \tag{37}$$

Finally, the only unknown operators in (31) are $v_\perp^{\pm k}$, which are contained in $p_t^{\pm k}$ and $H_t^{\pm k}$. These will be determined from the heavy-light orbital angular momentum equation as in the spinless RFT model [8]. From

$$\left[\frac{L}{r} = \frac{1}{2}\{W_r, \gamma_\perp v_\perp\} + a\{r, F(v_\perp)\}\right] \Psi(\mathbf{r}) \ , \tag{38}$$

and using $L\mathcal{Y}_{jm}^k(\hat{\mathbf{r}}) = \sqrt{k(k+1)}\mathcal{Y}_{jm}^k(\hat{\mathbf{r}})$, one immediately finds equations that determine the $v_\perp^{\pm k}$ operators:

$$\left[\frac{\sqrt{k(k+1)}}{r} = \tfrac{1}{2}\{W_r, \gamma_\perp^k v_\perp^k\} + a\{r, F(v_\perp^k)\}\ \right] f_j^k(r)\mathcal{Y}_{jm}^k(\hat{\mathbf{r}}) \ , \tag{39}$$

$$\left[\frac{\sqrt{-k(-k+1)}}{r} = \tfrac{1}{2}\{W_r, \gamma_\perp^{-k} v_\perp^{-k}\} + a\{r, F(v_\perp^{-k})\}\ \right] g_j^k(r)\mathcal{Y}_{jm}^{-k}(\hat{\mathbf{r}}) \ . \tag{40}$$

The numerical technique used to solve for $v_\perp$ is discussed in detail elsewhere [1, 8].

4 Semi-relativistic reduction

For comparison with previous results we decouple (31) and make the non-relativistic reduction to order $(v/c)^4$ (ignoring the short-range V(r) component),

$$\begin{aligned} H = E_q &= m + \frac{1}{2E_0^+}\Big[(E_0^+ + m)H_t^k(E_0^+ + m) + (E_0^+ + m)T_t D_+ \\ &- D_- T_t(E_0^+ + m) - D_- H_t^{-k} D_+\Big]\frac{1}{2E_0^+} - \frac{D_- D_+}{E_0^+ + m} \\ &+ \frac{1}{2E_0^+}\Big[-(E_0^+ + m)H_t^k D_- D_+ + (E_0^+ + m)T_t(E_0^- - m)D_+ \\ &+ D_- T_t D_- D_+ - D_- H_t^{-k}(E_0^- - m)D_+\Big]\frac{1}{2E_0^+(E_0^+ + m)} \ . \end{aligned} \tag{41}$$

From (9) and (10) we find (with $L \simeq m v_\perp r$)

$$H_t \simeq ar + \frac{1}{6}arv_\perp \simeq ar + \frac{aL^2}{6m^2 r} \ , \tag{42}$$

$$p_t \simeq \frac{1}{3}arv_\perp \simeq \frac{aL}{3m} \ , \tag{43}$$

and from (41) it then follows

$$\begin{aligned} H &\simeq m - \frac{D_- D_+}{2m} - \frac{D_- D_+ D_- D_+}{8m^3} + H_t^k \\ &+ \frac{1}{4m^2}\Big(D_- D_+ H_t^k - D_- H_t^{-k} D_+\Big) - \frac{1}{2m}\Big(D_- T_t - T_t D_+\Big) \ . \end{aligned} \tag{44}$$

Taking expectation values, and using

$$k(k+1) \rightarrow L^2 \ , \tag{45}$$

$$-(k+1) \rightarrow 2\mathbf{S}\cdot\mathbf{L} \ , \tag{46}$$

$$D_- D_+ \rightarrow -p^2 \ , \tag{47}$$

we obtain the effective Hamiltonian

$$H = m + \frac{p^2}{2m} - \frac{p^4}{8m^3} + ar - \frac{a}{6m^2}\frac{\mathbf{S}\cdot\mathbf{L}}{r} - \frac{a}{6m^2}\frac{L^2}{r} - \frac{a}{12m^2 r} \ . \tag{48}$$

Physical interpretation can be established for each of the terms of the above effective Hamiltonian. The first three terms result from the expansion of the relativistic energy $\sqrt{p^2+m^2}$, and the fourth is the static tube energy. The spin-orbit terms is the net result of the kinematic Thomas precession and tube energy and momentum contributions. As already mentioned, our result differs from the one conventionally found from QCD [6].

The L^2 term in (48) has a nice interpretation as pointed out previously [4]. The tube's explicit contribution to the angular momentum is the sixth term of (48). There is also a hidden contribution from the $p^2/2m$ term. The rotational part of $\mathbf{p}$ yields to leading tube order ($p_t \ll p_q$)

$$\begin{aligned} \frac{p^2}{2m} &\simeq \frac{p_q^2}{2m} + \frac{p_q}{m}\frac{L_t}{r} \\ &= \frac{p_q^2}{2m} + (\frac{L}{mr})(\frac{aL}{3m}) \ , \end{aligned} \tag{49}$$

where we have used $L \simeq p_q r$ and $L_t/r \simeq aL/3m$ from (43). The total tube contribution to the L^2 part of the Hamiltonian is then

$$\Delta H_t = \frac{aL^2}{m^2 r}(\frac{1}{3} - \frac{1}{6}) = \frac{aL^2}{6m^2 r} \ . \tag{50}$$

The above is exactly the rotational energy of a rod of a mass ar and length r rotating with angular velocity $\omega = L/mr^2$,

$$\begin{aligned} E_t^{rot} &= \frac{1}{2}I\omega^2 \\ &= \frac{1}{2}(\frac{1}{3}ar)r^2\frac{L^2}{m^2 r^4} = \frac{aL^2}{6m^2 r} \ . \end{aligned} \tag{51}$$

The final term in (48) is a Darwin like term and it is sensitive to how the Hamiltonian is symmetrized. If one symmetrizes at the end as in previous work [3, 5], a different result is obtained.

5 Regge structure

A confined particle in a sufficiently large angular momentum state moves ultra relativistically. For linear confinement we expect linear Regge trajectories from classical considerations [8, 17]. In the flux tube model the angular momentum and rotational energy of the quark are negligible compared to those of the tube. The slope of the Regge trajectory can be found from the model without a detailed solution of the wave equation. To determine the Regge slope directly from the no-pair tube equation we note from (3) and (30) that ($m \to 0,\ p_r \to 0,\ v_\perp \to 1$)

$$p_t^k \xrightarrow{|k|\gg 1} \frac{|k|}{r} , \tag{52}$$

$$T_t \xrightarrow{|k|\gg 1} -\hat{k} p_t , \tag{53}$$

with $\hat{k} = \frac{k}{|k|}$ being the sign of k, while from (9) it follows

$$H_t^k \xrightarrow{|k|\gg 1} \frac{ar\pi}{2} . \tag{54}$$

We also have

$$E_0^\pm \xrightarrow{|k|\gg 1} p_t , \tag{55}$$

$$\lambda^\pm \xrightarrow{|k|\gg 1} \frac{1}{2} , \tag{56}$$

so that in the limit $|k| \gg 1$ we obtain

$$\mathbb{h}_0 \xrightarrow{|k|\gg 1} p_t \begin{pmatrix} 0 & \hat{k} \\ \hat{k} & 0 \end{pmatrix} , \tag{57}$$

$$\mathbb{L} \xrightarrow{|k|\gg 1} \frac{1}{2} \begin{pmatrix} 1 & \hat{k} \\ \hat{k} & 1 \end{pmatrix} , \tag{58}$$

$$\mathbb{I} \xrightarrow{|k|\gg 1} \begin{pmatrix} H_t & -\hat{k} p_t \\ -\hat{k} p_t & H_t \end{pmatrix} . \tag{59}$$

Multiplying out $\mathbb{L}\mathbb{I}\mathbb{L}$ then yields

$$E_q = \mathbb{L}\mathbb{I}\mathbb{L} + \mathbb{h}_0 \simeq \frac{1}{2}\begin{pmatrix} H_t - p_t & (H_t + p_t)\hat{k} \\ (H_t + p_t)\hat{k} & H_t - p_t \end{pmatrix} . \tag{60}$$

Independent of the sign of $\hat{k}$, the eigenvalues of (60) are

$$E_{q+} = H_t \simeq \frac{ar\pi}{2} , \tag{61}$$

$$E_{q-} = -p_t \simeq -\frac{|k|}{r} . \tag{62}$$

The positive energy solution has the proper Regge behavior. From (38) we find the total orbital angular momentum of the system in the ultra-relativistic limit to be

$$L \stackrel{|k|\gg 1}{\longrightarrow} \frac{a\pi r^2}{4} \simeq |k| . \tag{63}$$

Eliminating r and using (61) we obtain the ratio of angular momentum to the square of the energy of the light degrees of freedom,

$$\frac{|k|}{E_q^2} \stackrel{|k|\gg 1}{\longrightarrow} \frac{1}{\pi a} . \tag{64}$$

This is the same slope that one would obtain from a Nambu string with one end fixed.

6 Numerical results

By expanding f_j^k and g_j^k in terms of a complete set of basis states, and then truncating the expansion to the first N states we can transform the angular momentum equations (39-40) into two $N \times N$ matrix equations from which matrices for $v_\perp^{\pm k}$ operators are found [8]. Also, the radial no-pair equation becomes a $2N \times 2N$ matrix equation, which we solve using the Galerkin variational method. The quasi-Coulombic basis states (which depend on a scale parameter β), and all matrix elements used are described in [11]. In Fig. 1 we show the dependence on β for the three lowest positive and three highest negative energy states, with the particular choice $m = 0.3\ GeV,\ k = -1,\ j = \frac{1}{2},\ a = 0.2\ GeV^2$, and $\kappa = 0.5$. As we increase the number of states N, the plateau where the positive eigenvalues are stable enlarges.

The Regge slope of the no-pair equation with the flux tube was shown in Section 5 to be $\alpha' = \frac{1}{\pi a}$. Our numerical solution agrees as shown in Fig. 2. In this figure we illustrate the leading trajectories for the two light degrees of freedom parity states corresponding to $k = \pm(j + \frac{1}{2})$ for $m_{u,d} = 0.3\ GeV,\ a = 0.2\ GeV^2$ and $\kappa = 0.5$. We also show several daughter trajectories corresponding to radial excitations.

In order to recover the universal Regge slope, we fix a to be $0.2\ GeV^2$, and we also choose $m_{u,d} = 0.3\ GeV$ and fit to the spin averaged heavy-light meson states. Our result is shown in Table 1, and parameters of the fit are

$$\begin{aligned} m_{u,d} &= 0.300\ GeV\ (\text{fixed})\ , \\ m_s &= 0.581\ GeV\ , \\ m_c &= 1.286\ GeV\ , \\ m_b &= 4.621\ GeV\ , \\ a &= 0.200\ GeV^2\ (\text{fixed})\ , \\ \kappa &= 0.641\ . \end{aligned} \tag{65}$$

The agreement of the fitted levels to experiment is excellent, all spin-averaged states are reproduced with errors of about 5 MeV.

Finally we use the wavefunctions with parameters of (65) to evaluate the Isgur-Wise function for the semileptonic $\bar{B} \to D^{(*)} l \bar{\nu}_l$ decays using [18]

$$\xi(\omega) = \frac{2}{\omega + 1} \langle\ j_0(2E_q \sqrt{\frac{\omega - 1}{\omega + 1}} r) \rangle\ , \tag{66}$$

where

$$\langle A \rangle = \int_0^\infty dr\ r^2 R(r) A(r) R(r)\ . \tag{67}$$

As shown on the Fig. 3, the agreement with ARGUS [20] and CLEO II [21] data is excellent. For the seven CLEO II data points, this IW function has χ^2 per degree of freedom of 0.4 (corresponding to about 90% CL). To calculate the slope, we use [19] expression

$$\xi'(1) = -(\frac{1}{2} + \frac{1}{3}E_q^2\langle r^2\rangle) \ . \tag{68}$$

For the light quark mass of 300 MeV, and using values for a and κ from (65) we find

$$\xi'(1) = -1.26 \ . \tag{69}$$

We observe that slopes calculated from the different versions of the no-pair equation (with vector confinement [11] or with the flux tube) are more negative ($\xi'(1)$ ranging from about -1.2 to -1.3) than the ones calculated from the spinless RFT model or the Dirac equation with scalar confinement ($\xi'(1) \simeq -0.9$).

7 Conclusions

In this paper we further explore an idea [5] for describing the relativistic quantized system of a flux tube with fermionic quarks at its ends. We work out in detail the simplest case where one fermion has infinite mass. Our technique for incorporating the tube into the reduced Salpeter equation is the covariant flux tube transformation (16). In order to achieve a satisfactory description of a heavy-light system, there are two physical requirements that have to be satisfied:

1. In the ultrarelativistic limit the tube dynamics must dominate giving a Nambu string limit.

2. The semi-relativistic corrections must agree with rigorous QCD expectations.

This model meets the above requirements with the possible exception of the spin-orbit interaction.

Let us briefly review the evidence concerning the QCD spin-orbit interaction. The conventional wisdom is that the spin-orbit effective Hamiltonian is equivalent to pure Thomas precession implying a coefficient $-\frac{1}{2}$ instead of $-\frac{1}{6}$ in the $\mathbf{S}\cdot\mathbf{L}$ term of (48). The analysis of Eichten and Feinberg [2] does not say what the spin-orbit coefficient is although later work by Gromes [6] and the Milan group [3], with further assumptions, find the Thomas result. We believe this remains an open question.

The model also yields the expected Regge structure. For large angular momentum a Regge slope of $\alpha' = \frac{1}{\pi a}$, characteristic for a Nambu string with one fixed end, is obtained. A sequence of parallel equally spaced daughter trajectories follows from radial excitations of the quark. By varying the tension a, the Coulomb coefficient κ and the quark masses we can account for the known spin-averaged heavy-light levels. In Table 1 we show a fit with the light quark mass and the tension fixed at reasonable values. We also used the s-wave wave function to compute the Isgur-Wise function. The result agrees well with the known experimental data, as shown in Fig. 3.

The numerical techniques developed for the flux tube model with spinless quarks [1, 8] can be directly applied in the fermionic case since quantization of the orbital angular momentum sector is independent of the spin part. The extension to arbitrary two fermion systems seems to be free of any intrinsic difficulties.

ACKNOWLEDGMENTS

This work was supported in part by the U.S. Department of Energy under Contract Nos. DE-FG02-95ER40896 and DE-AC05-84ER40150, the National Science Foundation under Grant No. HRD9154080, and in part by the University of Wisconsin Research Committee with funds granted by the Wisconsin Alumni Research Foundation.

References

[1] D. LaCourse and M. G. Olsson, Phys. Rev. D **39**, 2751 (1989).

[2] E. Eichten and F. Feinberg, Phys. Rev. D **23**, 2724 (1981).

[3] A. Barchielli, E. Montaldi and G. M. Prosperi, Nucl. Phys. B **296**, 625 (1988); **303**, 752(E) (1988); A. Barchielli, N. Brambilla and G. M. Prosperi, Nuovo Cim. A **103**, 59 (1989); N. Brambilla, P. Consoli and G. M. Prosperi, Phys. Rev. D **50**, 5878 (1994); N. Brambilla and G. M. Prosperi, Phys. Lett. B **236**, 69 (1990).

[4] C. Olson, M. G. Olsson and K. Williams, Phys. Rev. D **45**, 4307 (1992).

[5] M. G. Olsson and K. Williams, Phys. Rev D **48**, 417 (1993). The result for $\mathbf{h}_i$ in Eq. (19) is incorrect. The corrected result agrees with the present paper.

[6] D. Gromes, Z. Phys. C **22**, 265 (1984); **26**, 401 (1984).

[7] C. Olson, M. G. Olsson and D. LaCourse, Phys. Rev. D. **49**, 4675 (1994).

[8] M. G. Olsson and S. Veseli, Phys. Rev. D **51**, 3578 (1995).

[9] A. Yu. Dubin, A. B. Kaidalov, and Yu. A. Simonov, Phys. Lett. B **323**, 41 (1994).

[10] E. L. Gubankova and A. Yu. Dubin, Phys. Lett. B **334**, 180 (1994).

[11] M. G. Olsson, S. Veseli, and K. Williams, Phys. Rev. D **51**, 5079 (1995).

[12] E. Salpeter, Phys. Rev. **87**, 328 (1952).

[13] A. Gara, B. Durand, and L. Durand, Phys. Rev. D **40**, 843 (1989).

[14] C. Long and D. Robson, Phys. Rev. D **27**, 644 (1983); W. Lucha, F. F. Schöberl and D. Gromes, Phys. Rep. **200**, 127 (1991).

[15] G. Hardekopf and J. Sucher, Phys. Rev. A **30**, 703 (1984); Phys. Rev. A **31**, 2020 (1985).

[16] F. Gross, *Relativistic Quantum Mechanics and Field Theory*, John Wiley & Sons, Inc., 1993.

[17] C. Goebel, D. LaCourse, and M. G. Olsson, Phys. Rev. D **41**, 2917 (1990).

[18] M. Sadzikowski and K. Zalewski, Z. Phys. C **59**, 677 (1993); H. Høgaasen and M. Sadzikowski, Z. Phys. C **64**, 427 (1994).

[19] M. G. Olsson and S. Veseli, Phys. Rev. D **51**, 2224 (1995).

[20] H. Albrecht et al., ARGUS Collaboration, Z. Phys. C **57**, 533 (1993).

[21] B. Barish et al., CLEO Collaboration, Phys. Rev. D **51**, 1014 (1995).

TABLES

Table 1: Heavy-light spin averaged states. Theoretical results are obtained from the no-pair equation with the flux tube. Spin-averaged masses are calculated in the usual way, by taking $\frac{3}{4}$ ($\frac{5}{8}$) of the triplet and $\frac{1}{4}$ ($\frac{3}{8}$) of the singlet mass for the s(p)-waves).

state	spectroscopic label J^P	$^{2S+1}L_J$	spin-averaged mass (MeV)	q. n. j	k	theory (MeV)	error (MeV)
$c\bar{u},\ c\bar{d}$ quarks							
D (1867)	0^-	$^1S_0$	$1S$ (1974)	$\frac{1}{2}$	-1	1980	6
D^* (2009)	1^-	$^3S_1$					
D_1 (2425)	1^+	$^1P_1$	$1P$ (2446)	$\frac{3}{2}$	-2	2440	-6
D_2^* (2459)	2^+	$^3P_2$					
$c\bar{s}$ quarks							
D_s (1969)	0^-	$^1S_0$	$1S$ (2076)	$\frac{1}{2}$	-1	2072	-4
D_s^* (2112)	1^-	$^3S_1$					
D_{s1} (2535)	1^+	$^1P_1$	$1P$ (2559)	$\frac{3}{2}$	-2	2563	4
D_{s2} (2573)	2^+	$^3P_2$					
$b\bar{u},\ b\bar{d}$ quarks							
B (5279)	0^-	$^1S_0$	$1S$ (5314)	$\frac{1}{2}$	-1	5315	1
B^* (5325)	1^-	$^3S_1$					
$b\bar{s}$ quarks							
B_s (5374)	0^-	$^1S_0$	$1S$ (5409)	$\frac{1}{2}$	-1	5408	-1
B_s^* (5421)	1^-	$^3S_1$					

FIGURES

Figure 1: Dependence on the basis state scale β of the three lowest positive energy states and the three highest negative energy states for the no-pair equation with flux tube. Here we have chosen $m_q = 0.3\ GeV,\ a = 0.2\ GeV^2,\ \kappa = 0.5,\ k = -1$ and $j = \frac{1}{2}$. The full lines correspond to $N = 25$, and dashed lines correspond to $N = 15$ basis states used.

Figure 2: Regge trajectories for the no-pair equation with flux tube. Again, we have chosen $m_{u,d} = 0.3\ GeV,\ a = 0.2 GeV^2$, and $\kappa = 0.5$. The full lines correspond to $k = -(j + \frac{1}{2})$, and dashed lines to $k = j + \frac{1}{2}$. To ensure that all calculated energies are correct, we used $N = 50$ basis states, and kept first 15 states.

Figure 3: The Isgur-Wise function for $\bar{B} \to D^{(*)} l \bar{\nu}_l$ decays calculated from the no-pair equation with tube confinement. Values for the light quark mass $m_{u,d}$, tension a and short range potential constant κ are taken from the fit (65). For the sake of clarity, error bars are shown only for the CLEO II data.

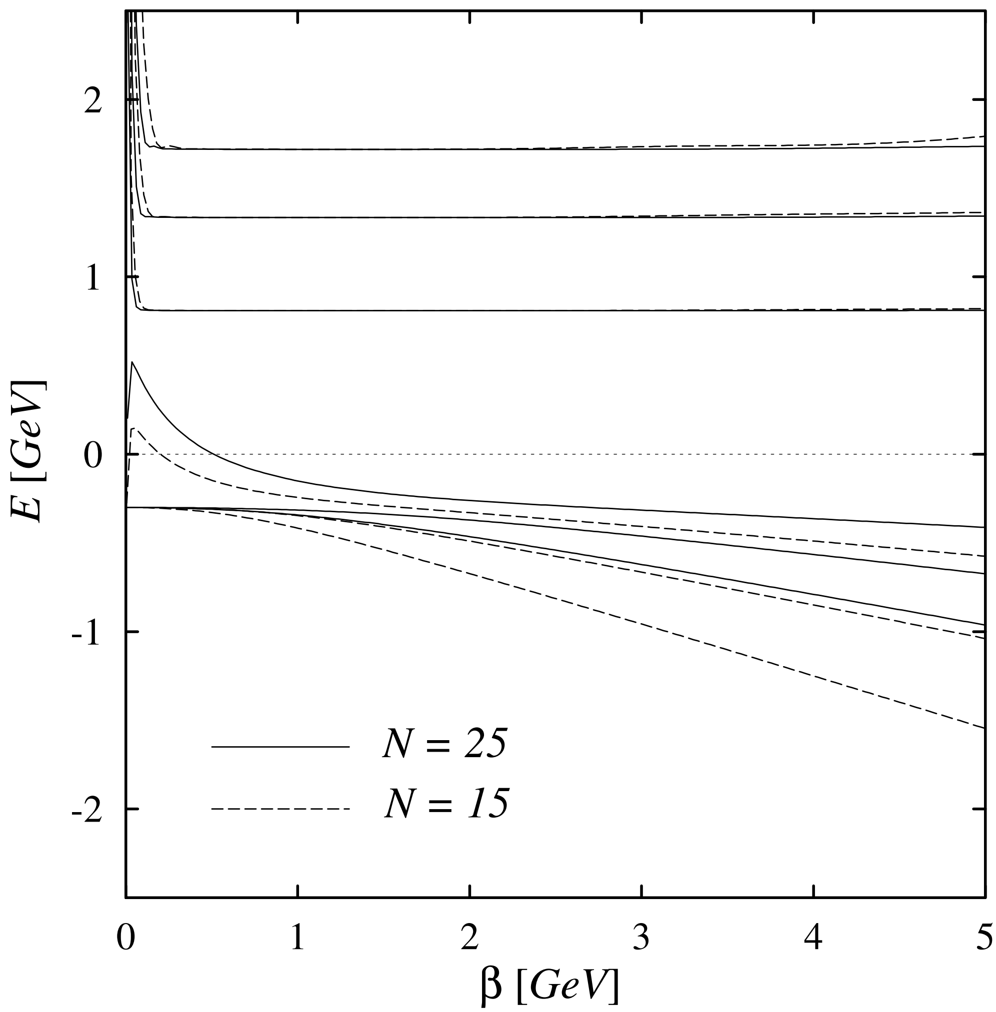

Figure 1

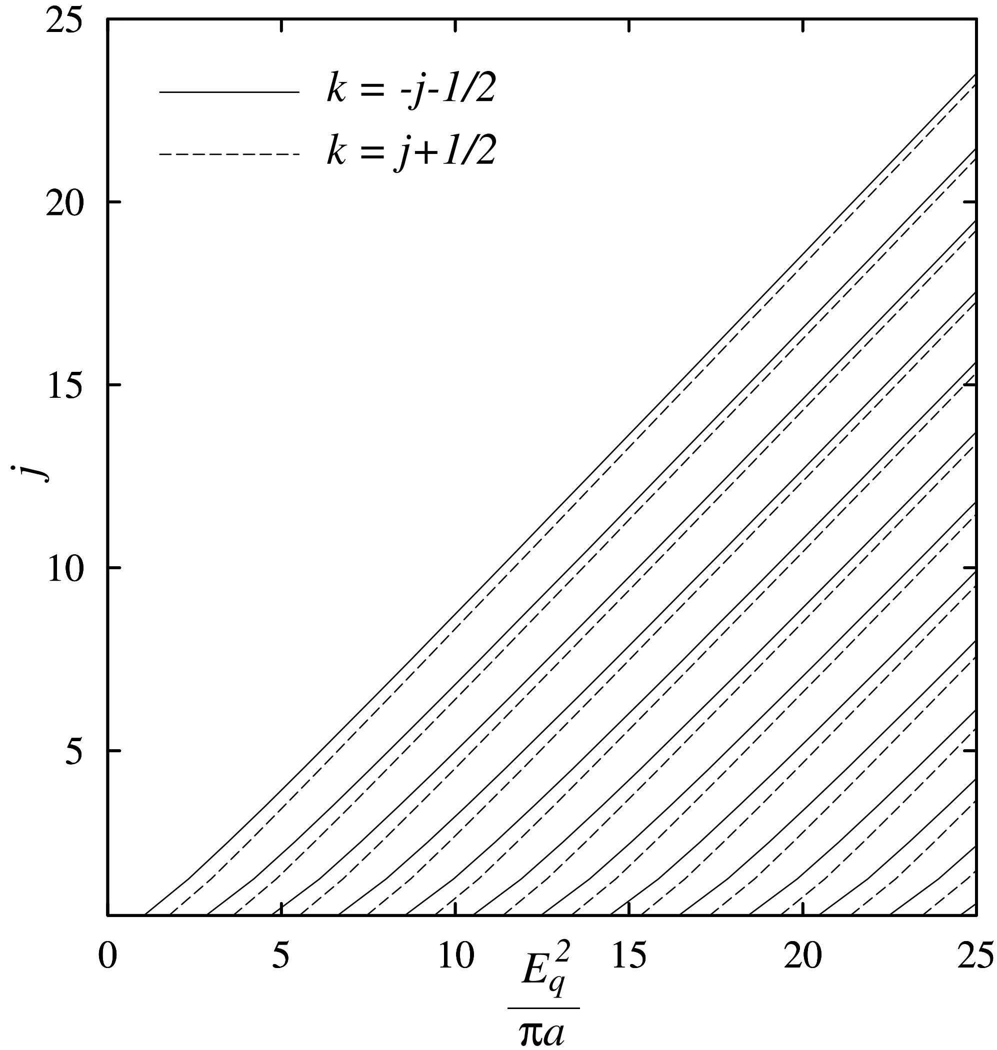

Figure 2

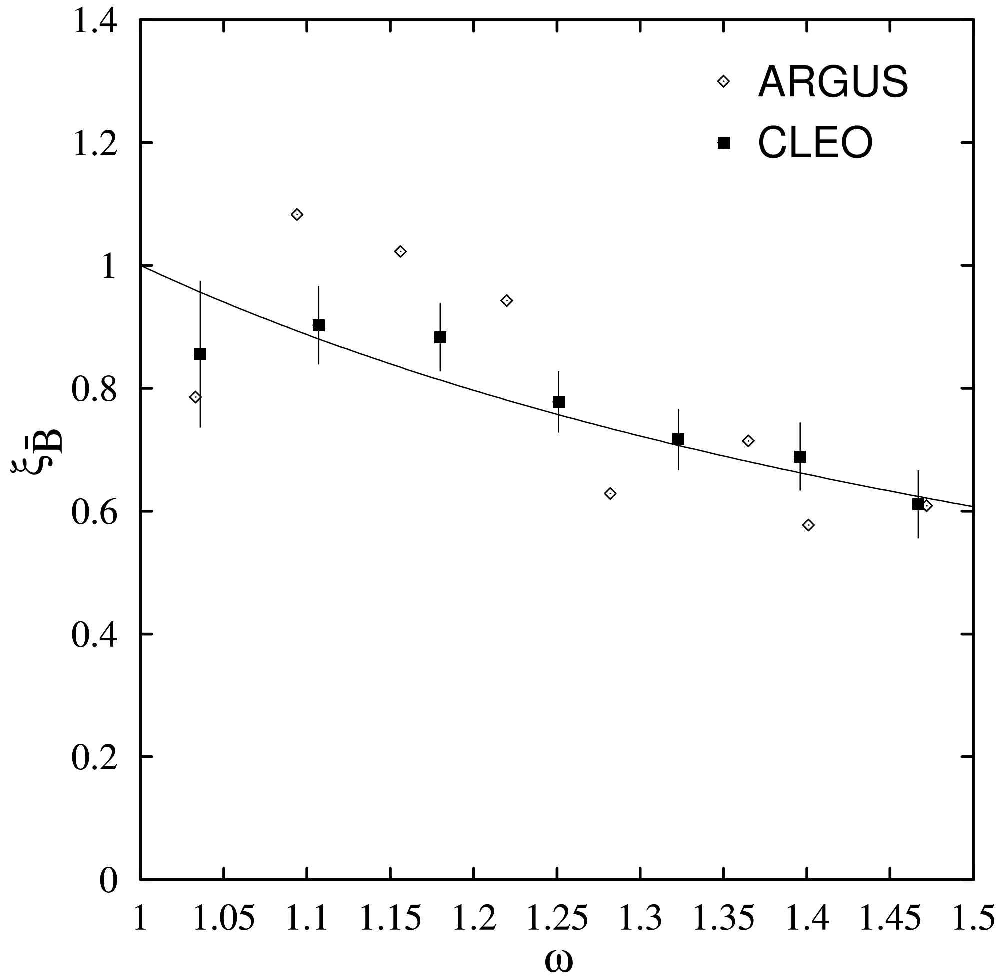
ARGUS
CLEO
1.4
1.2
1
0.8
0.6
0.4
0.2
0
1
1.05
1.1
1.15
1.2
1.25
1.3
1.35
1.4
1.45
1.5
$\xi_{\bar{B}}$
ω

Figure 3